INTERNAL REPORT #61
S. Hartman

INTER-OFFICE MEMO

CALIFORNIA INSTITUTE OF TECHNOLOGY

TO CRS Team

DATE 24 January 1975

FROM S. R. Hartman

SUBJECT PASSIVE COLLIMATOR STUDY

A study was done on the effectiveness of a passive collimator to eliminate the background in the LET L1 singles integral-analyzer, using a Monte Carlo calculation that included the energy loss in the collimator. The results of this study are summarized in the Appendix.

The conclusion is that for typical "1AU" spectra of H^1 and He^4 the collimator is useless. For these spectra the background is dominated by cosmic rays of energy greater than 150 Mev/n. This can be seen from Figure 3 and in the difference between Table I and Table II.

For a "Power-law" spectra of H^1, He^4 and O^{16} which were extropolated to low energies from the observed high energy spectra, the background due to cosmic rays of energy $\gtrsim$ 150 Mev/n is negligible. Table III shows that for this case the effect of a collimator does not increase the GOOD/BKGD ratio for protons. However, a 9.2 mil collimator does increase the ratio by a factor of ~ 2 for helium. This effect is not considered significant enough to require a collimator.

The L1 single - parameter analysis yields information on the cosmic ray spectra at energies below the threshold for the two-parameter analysis.

The thresholds for the integral analyzers are chosen to lower the contamination of the helium measurement by hydrogen, and the contamination by helium in the measurement of oxygen. The thresholds selected are: 0.38 Mev, to lower the counting rate for cosmic rays of energy greater than 150 Mev/n; 2.63 MeV for the H^1, He^4 boundary; 10.50 MeV for the He^4, O^{16} boundary, and 93.75 MeV for the O^{16}, Fe^{56} boundary.

SH/il

Attachments

APPENDIX

1. A "GOOD" particle is defined as a particle which stops in the detector, does not pass through a collimator, and has an energy loss in L1 below the two-parameter threshold.

   A background, "BKGD", particle is any particle not satisfying the criteria of a "GOOD" particle stated above.

2. An assumed 1 mg/cm^2 Mylar window was modeled by 6.4 μm of silicon. The collimator was assumed to be conical. Figure 1 shows a cross-section view of the LET telescope. Three thicknesses were used: 0.0 mil, equivalent to no collimator; 9.2 mil and 100.0 mil.

3. The spectra actually used in this calculation are plotted in Figure 2.

   The "1 AU" spectra are power-law approximations to typical observed cosmic ray spectra at 1 AU.

   The "Power Law" spectra are extensions to low energies of the spectra above ~ 2 Gev/n. The assumed power law is $\frac{dJ}{dT} = K\ T^{-2.65}$

and the coefficients are

	K $(cm^2\text{-sr-sec-Mev/n})^{-1}$	Ratio to H^1
H^1	7.96×10^4	1
He^4	1.14×10^4	1/7
O^{16}	1.59×10^2	1/500

4. Figure 3 shows the L1 singles counting rate/channel for the "1 AU" spectra case. The contributions of H^1 and He^4 to both "GOOD" and "BKGD" particles are plotted separately. The background due to cosmic rays of energy $\gtrsim$ 150 Mev/n is also plotted.

Notice that for all three thicknesses of the collimator the background due to cosmic rays of energy $\gtrsim$ 150 Mev/n dominates both the "GOOD" and "BKGD" contributions due to H^1 and He^4.

Excluding the background from cosmic rays of energy $\gtrsim$ 150 Mev/n, the ratios of GOOD/BKGD for particles within specified energy or channel intervals are tabulated in Table I for the "1 AU" spectra case. A collimator does not increase the ratio for H^1, but it does increase the ratio for He^4. However, when the background from cosmic rays of energy $\gtrsim$ 150 Mev/n is included, as listed in Table II, the ratios are not significantly increased as the thickness of the collimator is increased.

5. Figure 4 shows the L1 singles counting rate/channel for the "Power-law" spectra case. As in Figure 3, the contributions from H^1, He^4 and O^{16} are plotted separately. For the "Power-law" spectra case the background due to cosmic rays of energy $\gtrsim$ 150 Mev/n is negligible, since the number of particles below ~ 100 Mev/n has increased by a factor of ~ 10^7 in the "Power-law" spectra relative to the "1 AU" spectra.

The ratios of GOOD/BKGD within specified channel intervals for H^1, He^4 and O^{16} are listed in Table III for the "Power-law" spectra case. The ratios for H^1 do not change with the addition of a collimator. The ratio for He^4 increases by a factor of ~ 2 with the addition of a collimator, but this increase is not considered important enough to require a collimator.

6. The background due to cosmic rays of energy $\gtrsim$ 150 Mev/n was calculated in the following manner. All particles were assumed to be minimum ionizing, i.e. $\frac{dE}{dX} = z^2$ (0.4 Kev/μ). For a particular charge z, the range of path-lengths which contribute to a given energy interval was calculated. The geometrical factor for this range of path lengths was multiplied by the flux of the particle to get

the contribution to the counting rate in the energy interval. The contributions to each energy interval for charges z = 1 to z = 26 were summed. The integral flux for H^1 of energies $\gtrsim$ 150 Mev/n was taken to be 0.15 (cm^2-sr-sec).

7. The integral discriminator threshold for helium was chosen to minimize the background contribution from hydrogen. Figure 5 shows the ratio of the Good helium events to the Background events from background helium and all hydrogen. The input spectra used to calculate these curves were power laws of the form $T^{-\gamma}$, where γ = 2 in Figure 5 and 0.5 Mev/n $\leq$ T $\leq$ 150 Mev/n. The ratio of Good He^4/All Bkgd is plotted against the lower channel of the helium interval. Figure 6 shows these curves for γ = 3.

For all of the abundance ratios of He^4/H^1 shown, the best ratios of Good He^4/All Bkgd occur when the curves start leveling off at ~ 2.63 Mev.

Figure 7 and 8 show plots similar to Figures 5 and 6, but for helium and oxygen. The discriminator level for the He^4/O^{16} boundary is chosen to be 10.50 Mev.

For a single detector the average sec θ is 2.0. The energy needed to penetrate L1 for this pathlength is given in the following table:

PARTICLE	ENERGY TO PENETRATE 70μ of Si (Mev)
H^1	2.52
He^4	10.05
O^{16}	92.85

The integral discriminator thresholds chosen for hydrogen and for helium are slightly greater than these penetration energies. The integral discriminator threshold for oxygen was chosen to be 93.75 Mev using this penetration criteria.

TABLE I

RATIO OF GOOD/BKGD

FOR 1 AU SPECTRA

COLLIMATOR PARTICLE	CHANNEL INTERVAL (75 Kev/CH)		
	4-25	6-25	26-100
0.0 mil			
H^1	1.13	1.34	
He^4	0.087	0.11	0.76
9.2 mil			
H^1	0.69	0.81	
He^4	0.067	0.083	0.52
100 mil			
H^1	0.74	0.87	
He^4	0.068	0.090	3.33

TABLE II

RATIO OF GOOD/BKGD

FOR 1 AU SPECTRA

WITH BACKGROUND DUE TO

COSMIC RAYS OF ENERGY

$\gtrsim$ 150 Mev/n INCLUDED

COLLIMATOR PARTICLE	CHANNEL INTERVAL 4-25	6-25	26-100
0.0 mil			
H^1	0.491	0.616	
He^4	0.038	0.051	0.031
9.2 mil			
H^1	0.275	0.338	
He^4	0.027	0.035	0.128
100 mil			
H^1	0.283	0.349	
He^4	0.026	0.036	0.141

TABLE III

RATIO OF GOOD/BKGD

FOR POWER-LAW SPECTRA

COLLIMATOR PARTICLE	CHANNEL INTERVAL			
	4-25	6-25	26-100	101-1009
0.0 mil				
H^1	5.85	4.78		
He^4	0.72	0.65	1.31	
O^{16}	0.0040	0.0039	0.0083	0.102
9.2 mil				
H^1	5.43	4.29		
He^4	0.72	0.66	2.88	
O^{16}	0.0049	0.0047	0.024	0.746
100 mil				
H^1	5.85	4.75		
He^4	0.81	0.76	3.62	
O^{16}	0.0050	0.0050	0.028	3.19

TABLE IV

INCIDENT ENERGY NEEDED TO

PENETRATE PORTIONS OF THE LET TELESCOPE

	H^1		He^4		O^{16}	
TO PENETRATE	T (Mev/amu)	E (Mev)	T (Mev/amu)	E (Mev)	T (Mev/amu)	E (Mev)
WINDOW (1 mg/cm^2 of Ti)	0.24	0.24	0.16	0.64	0.17	2.79
WINDOW AND THRESHOLD FOR L1	0.41	0.41	0.26	1.03	0.22	3.47
WINDOW AND L1	1.70	1.72	1.70	6.80	4.08	65.18
WINDOW AND L1 AND THRESHOLD FOR L2	1.75	1.77				

FIGURE CAPTIONS

FIGURE 1 — Cross-section of the LET telescope with a collimator.

FIGURE 2 — Plots of the differential energy spectra for the "1 AU" spectra and the "Power-law" spectra.

FIGURE 3 — Plots of the counting rate/channel for the L1 singles pulse-height analysis mode, for the "1 AU" spectra case.

The separate contributions of H^1 and He^4 to "GOOD" particles and "BKGD" particles are shown.

Included is the plot of the background due to cosmic rays of energy $\gtrsim$ 150 Mev/n.

FIGURE 4 — Plots of the counting rate/channel for the L1 singles pulse-height analysis mode for the "Power-law" spectra case.

The separate contributions of H^1, He^4 and O^{16} to "GOOD" particles and "BKGD" particles are shown.

Included is the plot of the background due to cosmic rays of energy $\gtrsim$ 150 Mev/n.

FIGURE 5 Plots of the ratio Good He^4/All Bkgd versus the lower channel of the helium interval for various values of the abundance ratio He^4/H^1.

Input spectra are

$T^{-\gamma}$ for $\gamma = 2$ and

0.5 Mev/n $\leq T \leq$ 150 Mev/n

FIGURE 6 Similar to Figure 5 but for $\gamma = 3$.

FIGURE 7 Plots of the ratio Good O^{16}/All Bkgd versus the lower channel of the oxygen interval for various values of the abundance ratio O^{16}/He^4.

For $\gamma = 2$.

FIGURE 8 Similar to Figure 7 but for $\gamma = 3$.

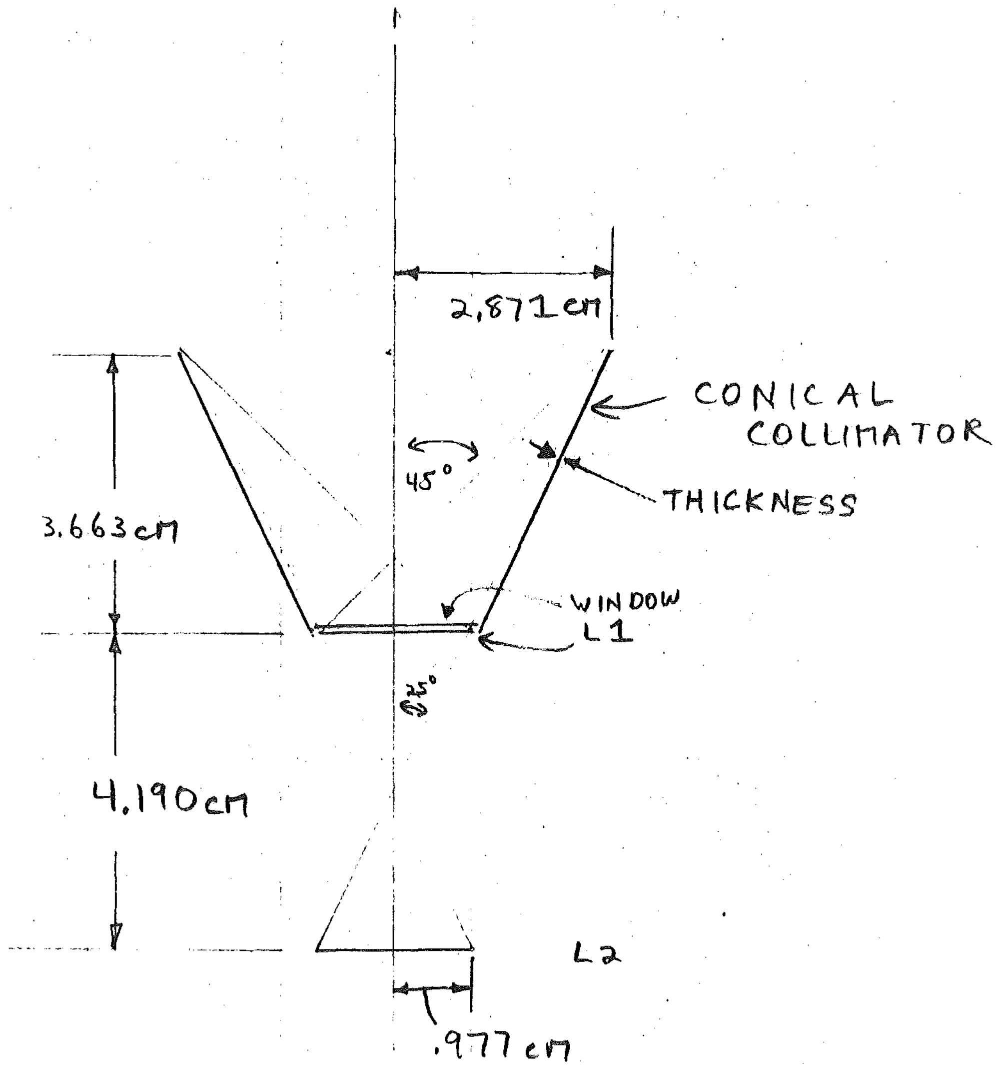

FIGURE 1

DRAWING OF LET TELESCOPE WITH COLLIMATOR

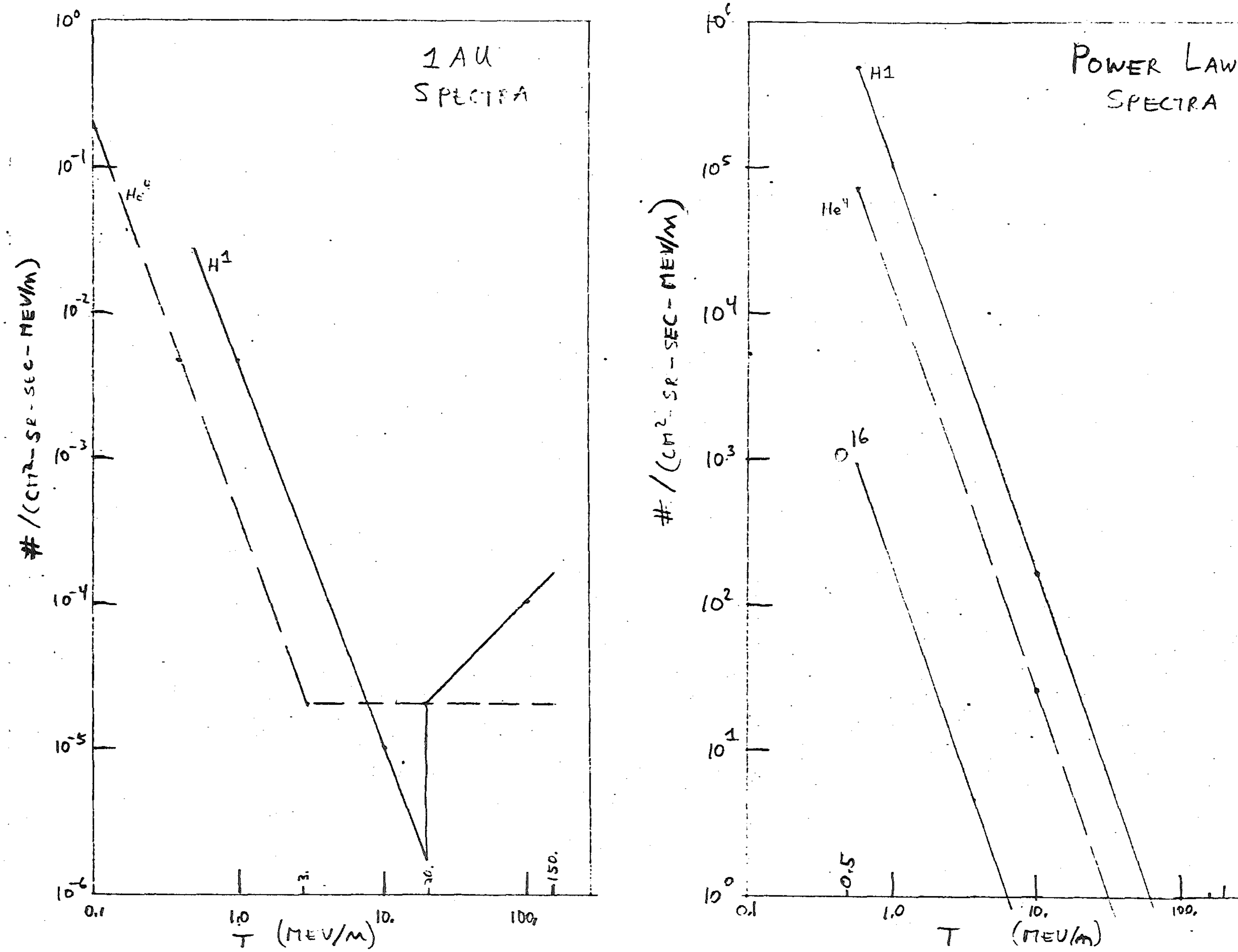

1 AU
SPECTRA
He4
H1
#/(CM2-SR-SEC-MEV/M)
10^0
10^-1
10^-2
10^-3
10^-4
10^-5
10^-6
0.1
1.0
3.
10.
20.
100.
150.
T (MEV/M)
POWER LAW
SPECTRA
H1
He4
O16
#/(CM2-SR-SEC-MEV/M)
10^6
10^5
10^4
10^3
10^2
10^1
10^0
0.1
0.5
1.0
10.
100.
T (MEV/M)

FIGURE 2

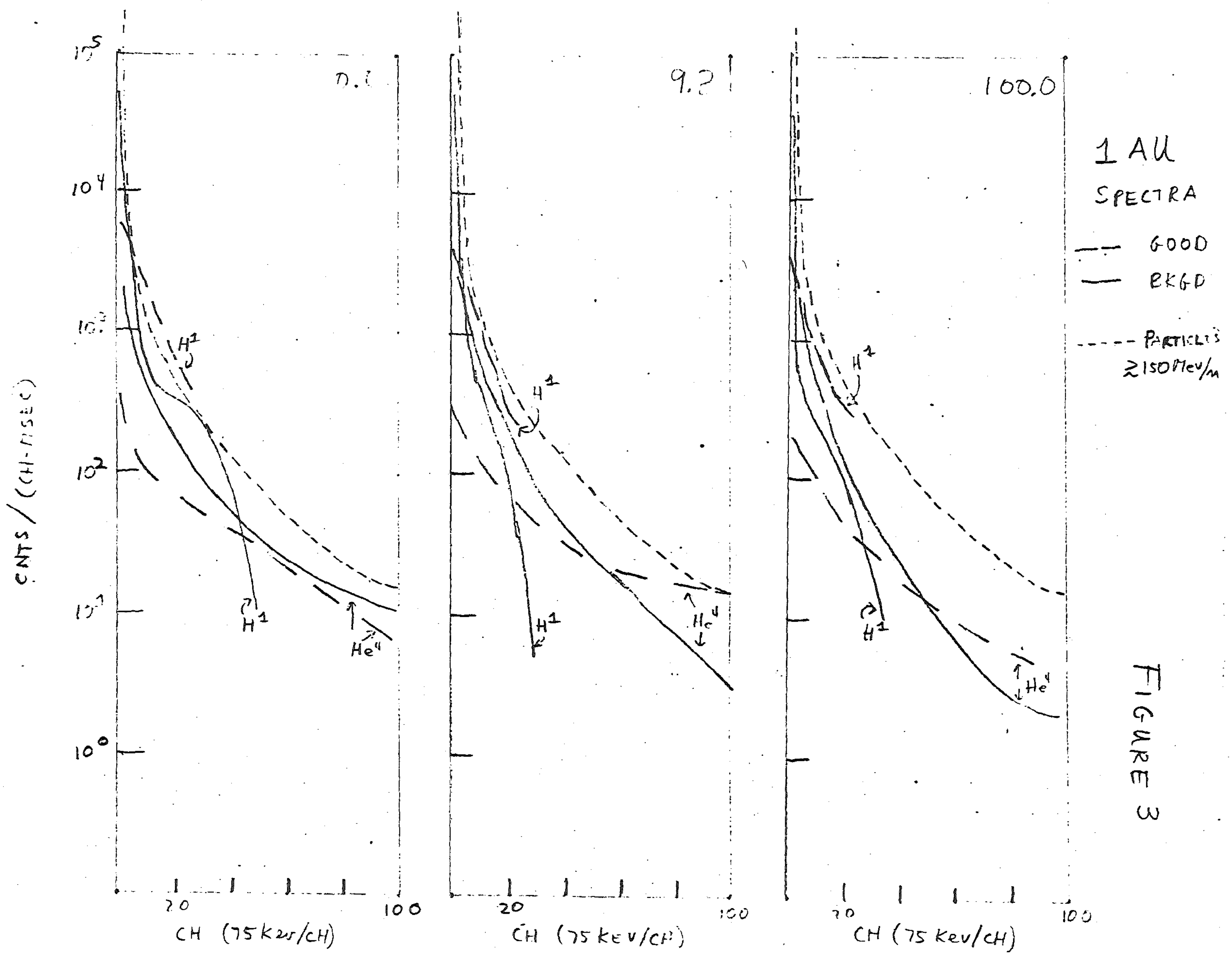

1 AU
SPECTRA
GOOD
BKGD
PARTICLES ≳150 MeV/M
9.2
100.0
CNTS / (CH-MSEC)
CH (75 keV/CH)
20
100
H1
He4

FIGURE 3

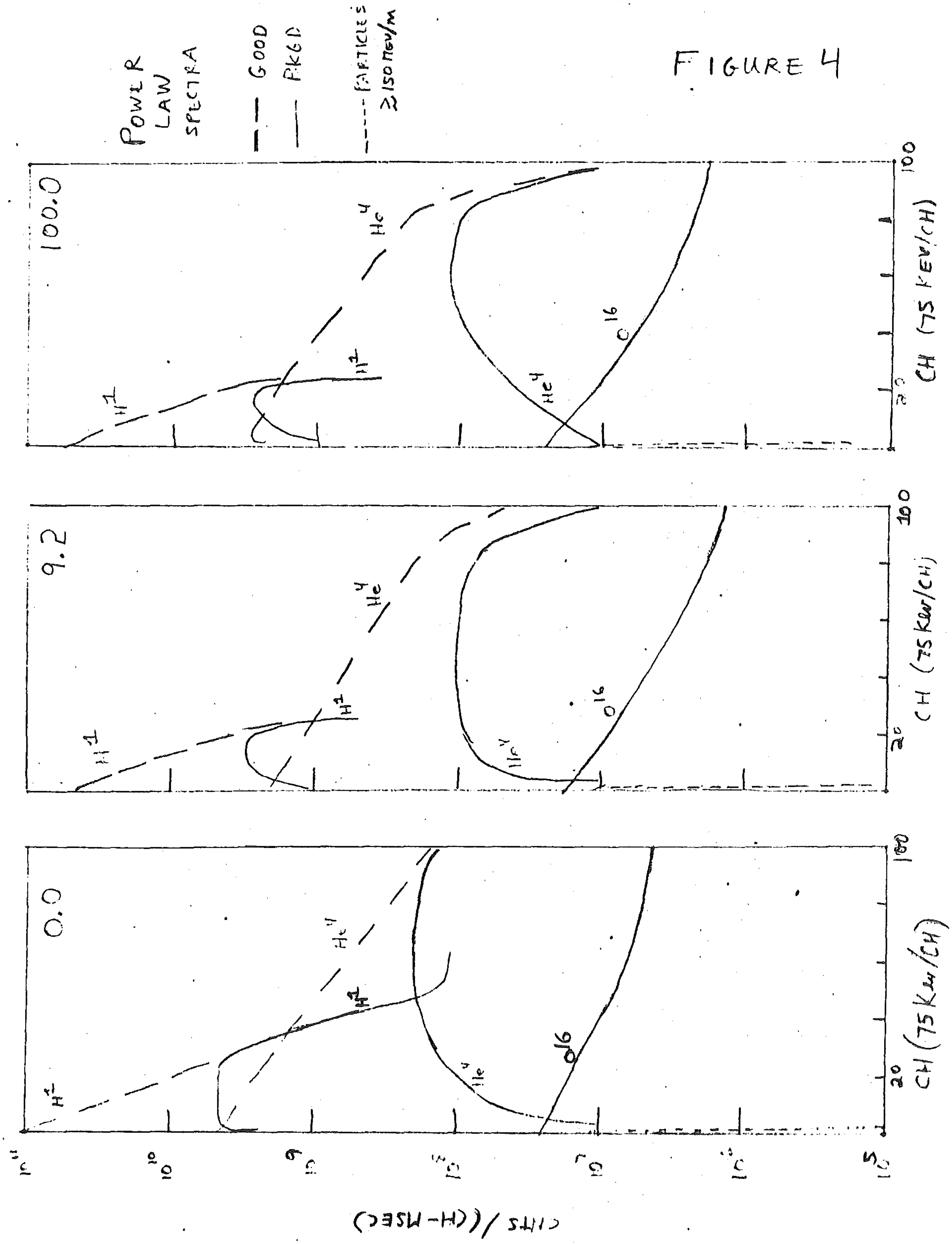
POWER LAW SPECTRA
GOOD
BKGD
PARTICLES ≥ 150 MeV/M
0.0
9.2
100.0
H1
He4
O16
CH (75 KeV/CH)
CTS / (CH-MSEC)

FIGURE 4

FIGURE 5

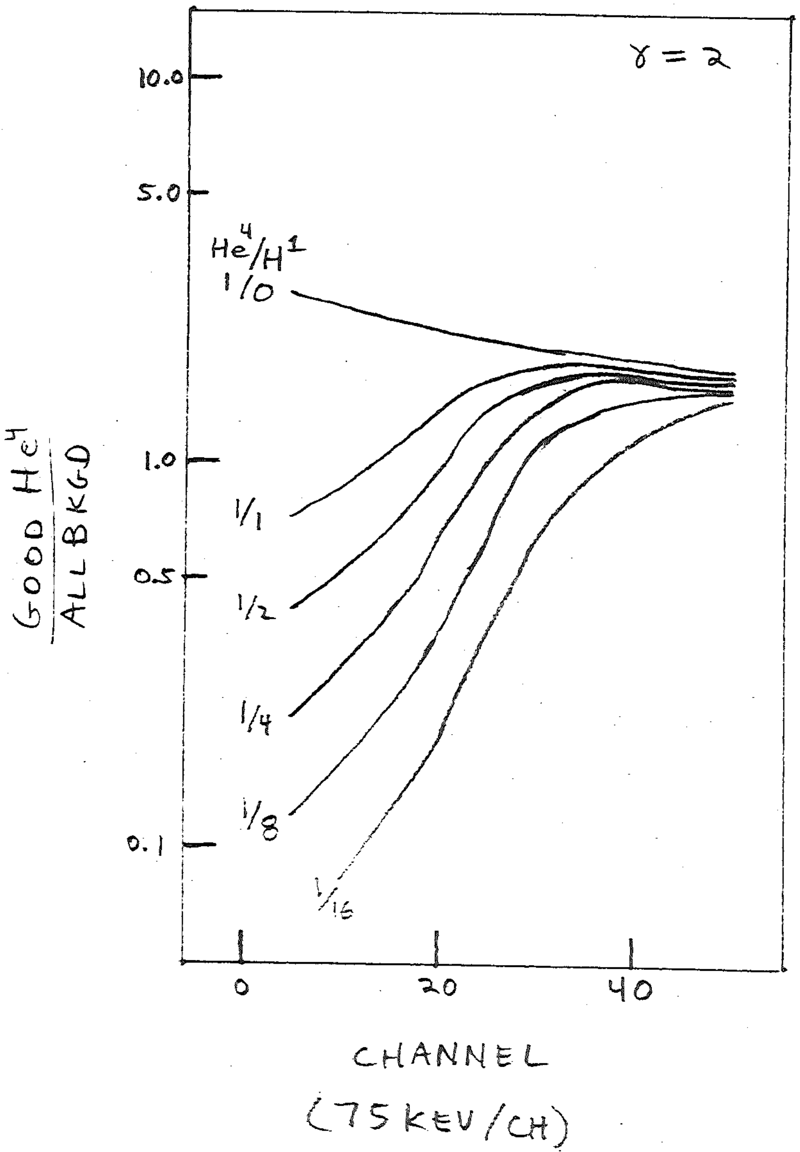

FIGURE 6

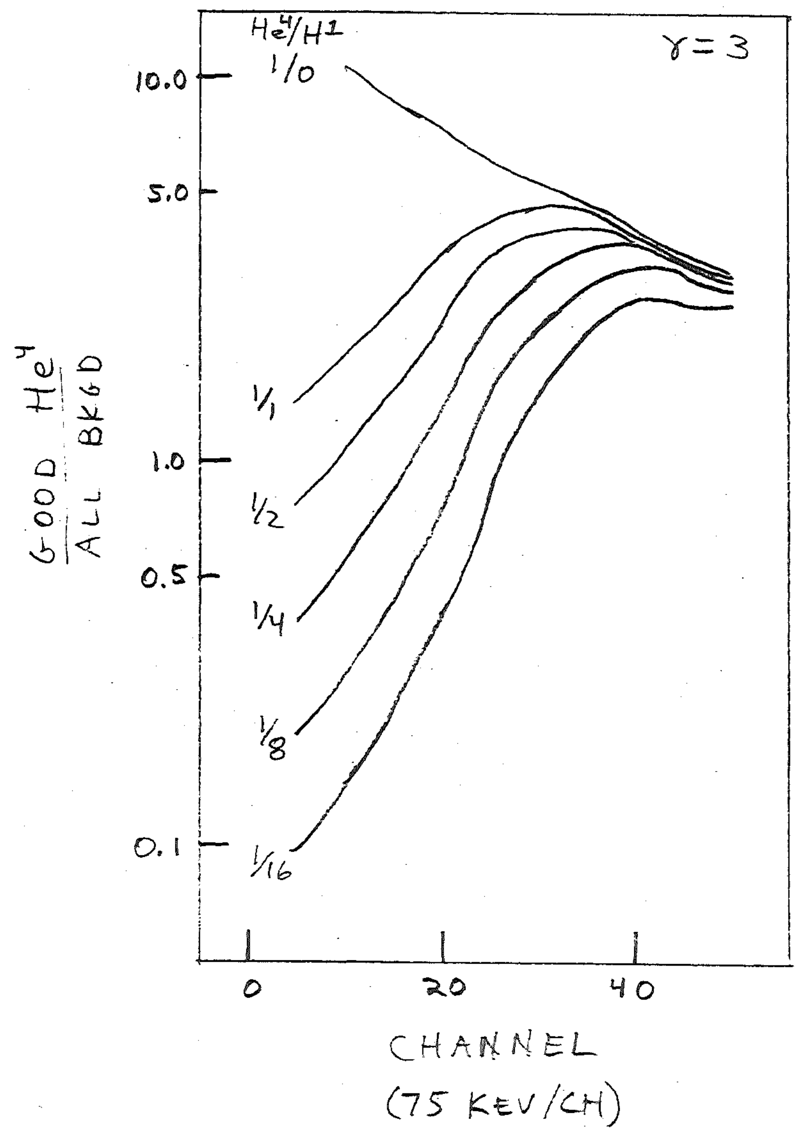

FIGURE 7

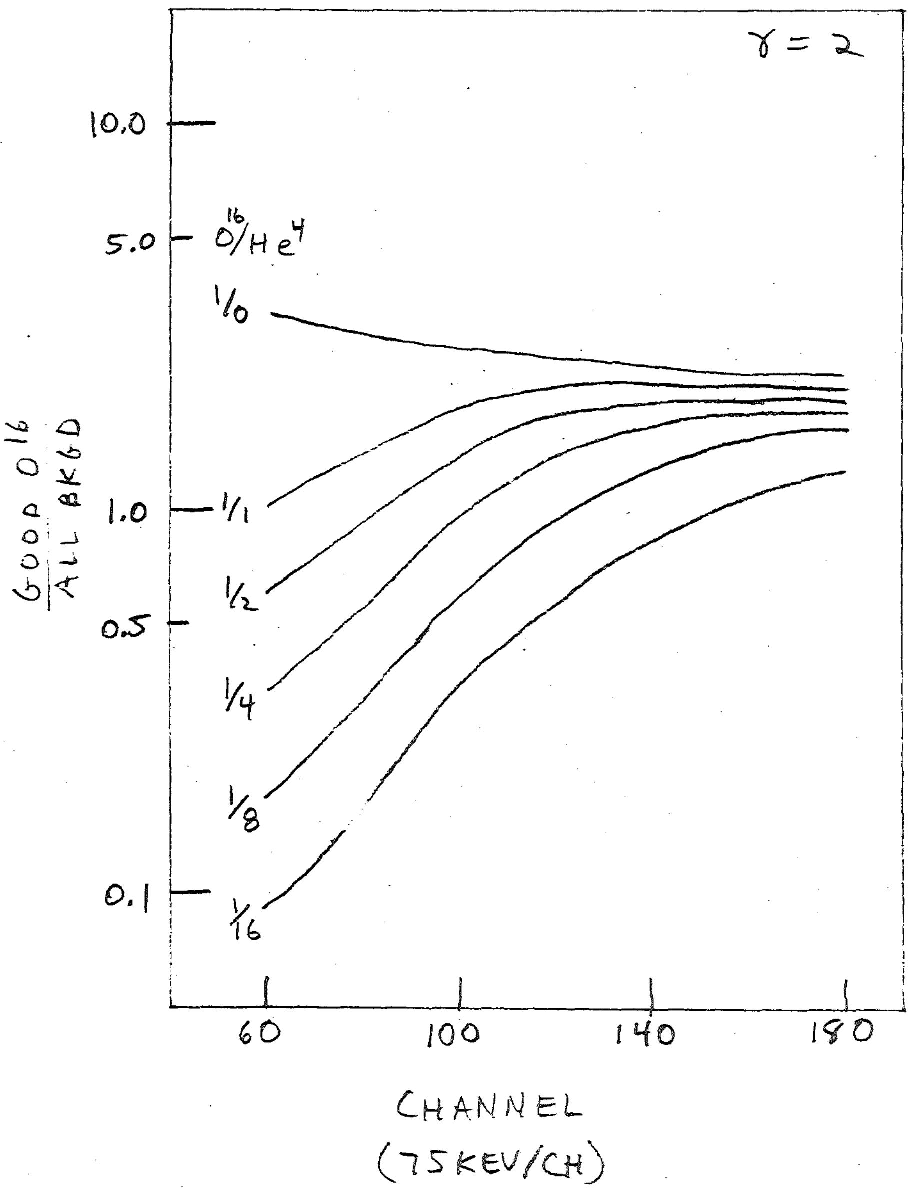

FIGURE 8

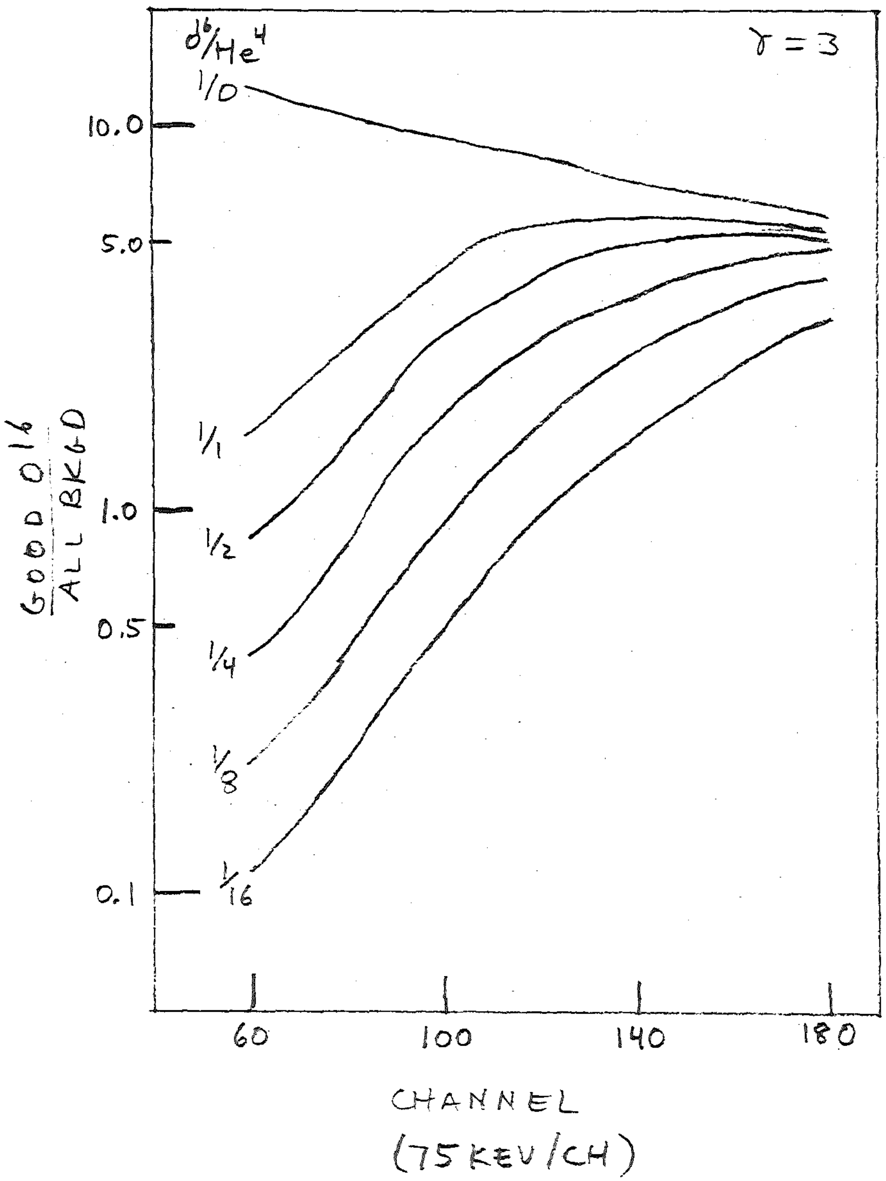

S. R. Hartman
July 17, 1975

ADDENDUM TO INTERNAL REPORT #61

Selection of Discriminator Thresholds

1. Each discriminator threshold was chosen to maximize the counting rate of the dominant particle species within each energy interval.

Below 0.38 MeV the penetrating particles of T > 150 MeV/n dominate. Between 0.38 MeV and 2.63 MeV "Good" H^1 dominates. For 2.63 MeV to 10.5 MeV Figures 5 and 6 show that He^4 dominates above 2.63 MeV (ch 35) and Figures 7 and 8 show that O^{16} dominates above 10.5 MeV (ch 140). The upper O^{16} threshold at 92.8 MeV was chosen because the O^{16} rate decreases sharply above this energy and the counting rate is due to particles with Z > 8 (e.g. Fe^{56}).

2. The rates obtained for each of these intervals are a mixture of "Good" particles for that energy interval and "All Background" particles whose energy loss in L1 falls within that interval. The ratio of "Good"/"All Bkgd." is a function of the elemental abundance and the actual spectra (as illustrated in Figures 5, 6, 7 and 8). This mixing forces any analysis of these rates to assume some reasonable spectra derived from dE/dx, total E analysis of L1 , L2 events and from the L1 singles, pulse height analysis.